Mon. Not. R. Astron. Soc. **000**, 1–8 (2006) Printed April 10, 2006 (MN LATEX style file v2.2)

Radial and rotational velocities of young brown dwarfs and very low-mass stars in the Upper Scorpius OB association and the ρ Ophiuchi cloud core

Ryuichi Kurosawa⋆ and Tim J. Harries
School of Physics, University of Exeter, Stocker Road, Exeter EX4 4QL

Dates to be inserted

ABSTRACT

We present the results of a radial velocity (RV) survey of 15 brown dwarfs (BDs) and very low-mass (VLM) stars in the Upper Scorpius OB association (UScoOB) and 3 BD candidates in the ρ Ophiuchi dark cloud core. We obtained high-resolution echelle spectra at VLT using Ultraviolet and Visual Echelle Spectrograph (UVES) at two different epochs for each object, and measured the shifts in their RVs to identify candidates for binary/multiple systems in the sample. We found 9 out of 18 (50 per cent) in our sample show a significant RV change in 4–33 d time scale, and are considered as binary/multiple 'candidates.' The fraction slightly decreases to 43 per cent (6 out of 14) if we consider the objects only in the UScoOB. These fractions do not necessary represent that of a real binary population among young BDs and VLM stars since their true multiplicities are still to be confirmed by follow-up spectroscopic monitoring. We found no double-lined spectroscopic binaries in our sample, based on the shape of cross-corelation curves. Our RV-shift tests successfully detected the recently confirmed 3 binaries in UScoOB via high-resolution imaging technique. We found the RV dispersion of the objects in UScoOB is very similar to that of the BDs and VLM stars in Chamaeleon I (Cha I) previously studied by others. We also measured the rotational velocities ($v \sin i$) of the sample, and found good agreements with earlier studies. The distribution of $v \sin i$ for the UScoOB objects peaks around $16.9\,\mathrm{km\,s^{-1}}$ which is similar to that of the Cha I population.

Key words: stars: binaries:spectroscopic – stars: low-mass, brown dwarfs – stars: formation – stars:planetary system: formation

1 INTRODUCTION

Most stars are member of binary systems and it is therefore important that a complete star formation theory be able to predict the binary fraction, period distribution, and mass-ratio distribution of newly born stellar objects across a wide range of masses. Furthermore, the study of the individual binary system is the only direct means to determine the fundamental stellar properties such as stellar masses and radii.

Recent high-resolution imaging studies of young brown dwarfs (BDs) and very low-mass (VLM) stars have placed strong constraints on binaries with separations of $\sim 1 - 100\,\mathrm{au}$. For example, Hubble Space Telescope (*HST*) observations of α Per and the Pleiades indicates a binary fraction (f) of > 10 per cent with a bias towards separations (a) of less than 15 au, and a mass-ratio (q) of > 0.7 (Martín et al. 2003) for objects around and below the hydrogen burning limit (see also Bouy et al. 2006). A similar lack of wide binaries was found in the field T-dwarf study (Burgasser et al. 2003), while $f = 15$ per cent was determined by Close et al. (2003) using the adaptive optics at Gemini North. They also found an upper limit to the semi-major axis distribution of $\sim 20\,\mathrm{au}$. An *HST* study of more than 80 field last M and L dwarfs (Gizis et al. 2003) indicated $f = 15$ per cent with separations in the range of 1.6–16 au. For s small sample (12) of BDs and VLM stars (0.04–0.1 $\mathrm{M}_{\odot}$) in Upper Scorpius OB association (UScoOB), Kraus et al. (2005) found $f = 25^{+16}_{-8}$ per cent for $5\,\mathrm{au} < a < 18\,\mathrm{au}$ by using a similar imaging technique..

Using a Monte Carlo simulation, the data from radial velocity surveys available in the literature, and by carefully considering the sensitivity and sampling biases, Maxted & Jeffries (2005) found an overall BD/VLM binary frequency of 32–45 per cent assuming $f = 15$ per cent for $a > 2.6$ au. A recent photometric study (Pinfield et al. 2003) of low-mass objects in Pleiades and Praesepe suggested, albeit indirectly, f as large as 50 per cent. which would only be compatible with direct imaging studies if 70–80 per cent of those binaries have $a < 1\,\mathrm{au}$. For a more comprehensive review

⋆ E-mail: rk@astro.ex.ac.uk

of the current status of BD/VLM binary fraction and the separation distribution, readers are refer to a recent review of multiplicity studies by Burgasser et al. (2006).

The extensive imaging surveys provide excellent observational constraints on wider BD+BD binaries, but it is now necessary to search for shorter period BD+BD binaries systematically. Binaries with the separation of less than 1 au are not resolved by current imaging techniques, but will be detectable as spectroscopic binaries, providing the mass-ratio is not too extreme, and velocity separation is large enough. The first BD+BD spectroscopic binary, PPl 15 (Basri & Martín 1999) showed a double-peaked cross-correlation function with a maximum velocity separation of $> 70\,\mathrm{km\,s^{-1}}$. The binary was found to have an eccentric orbit ($e = 0.4$) with a period of $\sim 5.8\,\mathrm{d}$. Basri & Martín (1999) suggested that the formation process of substellar objects is biased towards smaller separation binaries based on the short period of PPl 15 and the lack of Pleiades BD binaries with separations $> 40\,\mathrm{au}$. Note that the median separation of binaries with solar-type primaries is 30 au Duquennoy & Mayor (1991). Pioneering work on the RVs of BDs and VLMs are presented by Guenther & Wuchterl (2003), Kenyon et al. (2005) and Joergens (2006b) who found a several binary candidates; however, the orbital parameters and masses of binaries remains unknown because the follow-up spectroscopic monitoring is lacking or still being undertaken. In addition to the follow-up observations, the number of BDs and VLM star binary candidates needs to be increased in order to have better statistics on short-period binary parameters.

The separation distribution of BD/VLM binaries is critical to understanding their origin. There are two main models for the formation of BDs and VLM stars: first, they formed in a similar manner to higher mass stars, but from smaller-mass, denser molecular cloud core (e.g. Padoan & Nordlund 2002); second, BD/VLM objects have low masses because they are ejected from the dense core in which they form via dynamical interactions in multiple system, cutting off their accretion before they have reached stellar masses (Reipurth & Clarke 2001; Bate et al. 2002). Alternatively, there is a third model in which a free-floating BD or planetary-mass object can be formed in the process of the photo-evaporation (Whitworth & Zinnecker 2004) with the outer layers of a pre-stellar core ($\sim 0.2\,\mathrm{M_\odot}$) removed by the strong radiation pressure from the nearby massive OB stars before the accretion onto the protostar at core centre occurs.

Due to the dynamical interaction involved in the second model, BD/VLM binaries that survive are generally expected to have small separations. In the first model, wider binaries may be expected to be more common. Bate et al. (2002) suggested that close binaries ($a < 10\,\mathrm{au}$) do not form directly, but result from hardening of wider systems though a combination of dynamical interactions, accretion and interactions with circum-binary discs. If BD/VLM binaries have formed through such mechanisms, one would not expect to find binaries with 1–10 au separations without also finding many with separation < 1 au. If an absence/rarity of binaries with 1 au were found, it would support the idea that they are ejected quickly from multiple systems before they have undergone the interactions that shorten their periods.

Our immediate aim is to identify spectroscopic and close BD/VLM binaries using the high-resolution echelle spectroscopy at two epochs. This experiment is sensitive to VLM binaries with separations of < 0.1 au which corresponds to a period of $\sim 10\,\mathrm{d}$. A larger sample of candidates will enable us to measure the binary fraction of these short-period/close binaries (once confirmed), and address whether there is a significant population of 'hidden' VLM companions. The long term goal of this project to follow up the binary candidates found in this paper by spectroscopically monitoring them over different time scales, enabling us to obtain the radial velocity curves and their minimum masses.

In Section 2. we describe the observations and the data reduction. The results of radial velocity and rotational velocity ($v \sin i$) measurements are presented in Sections 3.1 and 3.1 respectively. We discuss the binary/multiplicity fraction indicated by our RV survey in Section 4, and give our conclusions in Section 5.

2 OBSERVATIONS

Our sample consists of 18 young, very low-mass objects: 15 objects in the Upper Scorpius OB association ($\mathrm{d} \approx 145\,\mathrm{pc}$, de Zeeuw et al. 1999) from the list of Ardila et al. (2000) and 3 objects in the ρ Ophiuchi cloud core ($\mathrm{d} \approx 150\,\mathrm{pc}$, de Zeeuw et al. 1997) from Luhman & Rieke (1999). The spectral type of the objects range between M5 and M8.5, and the age $<\sim 10\,\mathrm{Myr}$ (Luhman & Rieke 1999; Ardila et al. 2000; Muzerolle et al. 2003; Kraus et al. 2005). The sample is not complete, and the selection was solely based on brightness and the observability. The basic properties of the targets based on the literature is summarised in Table 2.

We obtained high-resolution spectra with the Kueyen telescope of VLT (Cerro Parnal, Chile) using the UVES echelle spectrograph. The observations were carried out between 2004 April 5 and 2005 (XXX?) May 15 in service mode. For each object, spectra were obtained at two different epochs separated by several (between 4 and 33 d). For each object at a given night, two separate spectra are obtained consecutively. This allows us to derive more reliable uncertainty estimates in the RV values of our targets (c.f. Joergens 2006b). The data were obtained using the red arm of UVES spectrograph with two mosaic CCDs (EEV + MIT/LL with 2k×4k pixels). The wavelength coverage of 6708 – 10,250 Å and the spectral resolution $R \approx 40,000$ were used. The slit width and length of 1" and 12" were used respectively with a typical seeing of 0.8".

The data were reduced via the standard ESO pipeline procedures for UVES echelle spectra. In summary, the data were corrected for bias, interorder background, sky background, sky emission lines and cosmic ray hits. They were then flattened, optimally extracted, and finally the different orders were merged. No binning was performed to achieve high resolution required for the RV measurements. The wavelength was calibrated using the Thorium-Argon arc spectra with a typical value of the standard deviation of the dispersion solution of 5 mÅ which corresponds to $0.2\,\mathrm{km\,s^{-1}}$ at the central wavelength 8600 Å. However, the autoguiding of the telescope keeps the star at the centre of the slit with about a tenth of the FWHM ($1\,\mathrm{km\,s^{-1}}$) which sets the upper limit for the systematic error in the RV measurements (Bailer-Jones 2004). The accuracy of the wavelength calibration will be demonstrated in the RV measurements of a RV standard in the following section. A typical signal-to-noise ratio (S/N) per wavelength bin of the spectra is about 15, and the heliocentric velocity correction was applied to the final spectra.

3 RESULTS

3.1 Radial velocities

The radial velocities of each object were determined by using the cross-correlation function of the object spectrum with that of a tem-

Table 1. Summary of known properties of the targets from literature: a. Luhman & Rieke (1999) (original list for ρ Oph), b. Ardila et al. (2000) (original list for UScoOB), c. Wilking et al. (1999), d. Muzerolle et al. (2003), e. Kraus et al. (2005), and f. Mohanty et al. (2005).

Object	Sp.	mass $[\mathrm{M}_\odot]$	RV $[\mathrm{km\,s^{-1}}]$	$v \sin i$ $[\mathrm{km\,s^{-1}}]$	Known multiple?
GY 5	M7[c]	0.07[d]	-6.3 ± 1.9[d]	16.8 ± 2.7[d]	no
GY 141	M8.5[a]	0.02[d]	...	6.0[f]	no
GY 310	M8.5[c]	0.08[a,d]	...	10.0[f]	no
USco 40	M5[b]	0.1[b]	...	37.5[f]	no
USco 53	M5[b]	0.1[b]	...	45.0[f]	no
USco 55	M5.5[b]	$0.10 + 0.07$[e]	...	12.0[f]	yes[e]
USco 66	M6[b]	$0.07 + 0.07$[e]	-4.4 ± 0.6[d]	27.5[f]	yes[e]
USco 67	M5.5[b]	0.10[e]	...	18.0[f]	no
USco 75	M6[b]	0.07[e]	-5.6 ± 1.1[d]	63.0[f]	no
USco 100	M7[b]	0.05[e]	-8.9 ± 0.6[d]	50.0[f]	no
USco 101	M5[b]	0.05[b]	...	...	no
USco 104	M5[b]	0.05[b]	...	16.0[f]	no
USco 109	M6[b]	$0.07 + 0.04$[e]	-3.8 ± 0.7[d]	6.0[f]	yes[e]
USco 112	M5.5[b]	0.1[e]	...	8.0[f]	no
USco 121	M6[b]	0.02[b]	-38.9 ± 1.0[d]	...	no
USco 128	M7[b]	0.05[e]	-3.0 ± 1.6[d]	0.0[f]	no
USco 130	M7.5[e]	0.04[e]	...	14.0[f]	no
USco 132	M7[b]	0.05[e]	-8.2 ± 1.1[d]	...	no

plate star which has a spectra type. By visual inspection, the wavelength ranges used for the cross-correlation calculations are chosen by avoiding the regions of spectra affected by the telluric lines, and defects and fringes (in near infrared) of the CCDs. The radial velocities of objects with respect to the template are obtained by measuring the location of the peak in the cross-correlation function which is fitted by the combination of two gaussian functions sharing their centres and a constant term (XXXX What does this mean?). LHS 49 (Proxima Cen, M5.5) was chosen as the template for this purpose. The radial velocity of the template object LHS 49 was obtained by measuring the wavelength shifts of the prominent photospheric absorption features K I $\lambda\lambda$7664.911, 7698.974. This gives us $\mathrm{RV_{LHS49}} = -22.6 \pm 0.5\,\mathrm{km\ s^{-1}}$, which is in good agreement with the earlier measurement of García-Sánchez et al. (2001) who found $\mathrm{RV_{LHS49}} = -21.7 \pm 1.8\,\mathrm{km\ s^{-1}}$. The heliocentric RV of each object can be then calculated by adding $\mathrm{RV_{LHS49}}$ with the RV of each object with respect to LHS 49. In the following measurements of the heliocentric radial velocities, our measurement ($\mathrm{RV_{LHS49}} = -22.6 \pm 0.5\,\mathrm{km\ s^{-1}}$) will be used for consistency.

Before applying the cross-correlation technique to out main targets, we have applied the technique to the radial velocity standard HD 140538 for which an high-accuracy RV measurement via the fixed-configuration, cross-dispersed échelle spectrograph Elodie (Baranne et al. 1996) is available. This was done so to ensure not only the validity of the cross-correlation technique, but also the validity of the wavelength calibration. In this test, we found the heliocentric $\mathrm{RV_{HD\,140538}} = 18.8 \pm 0.6\,\mathrm{km\ s^{-1}}$ which is in good agreement with the Elodie radial velocity measurement of $19.00 \pm 0.05\,\mathrm{km\,s^{-1}}$ (Udry et al. 1999).

The result of the heliocentric RV measurements (from two epochs for each object) is summarised in Table 2 along with the uncertainties. The table also lists the uncertainties in the 'relative' radial velocities (σ_{RRV}) which is the uncertainty of RV with respect to the template star. The two consecutive measurements of RVs (from same nights) are used to find the RV of the night, and their uncertainties are obtained from the standard deviations of the mean (σ_{RRV}) and the uncertainty of the template RV value (c.f. Joergens 2006b). (XXX What do you need to include the uncertainty in the template star measurement when we are looking for relative changes in the bd RVs?) The 'average' radial velocities ($\overline{\mathrm{RV}}$) of the two epochs are also given in the same table. The $\overline{\mathrm{RV}}$ values of the objects in UScoOB are consistent with the earlier measurements of Muzerolle et al. (2003) in Table 2, except for the values for USco 66 and USco 75. This is unsurprising since the former is a known binary (Kraus et al. 2005) and the latter is a non-constant RV object (a candidate for a multiple) found in the RV-shift test which will be discussed next.

For each object and for each RV measurement, the deviations (ΔRV) from the average RV are computed and summaries in Fig. 1 along with their uncertainties (σ_{RRV}) in order to aid the identification of multiplicity candidates. Note that in computing ΔRV we do not require the knowledge of absolute or the heliocentric radial velocities, but only the relative velocities (with respect to a template). We identify an object as a candidate when the $1\sigma_{\mathrm{RRV}}$ error bar from each RV measurement overlaps one another. Using this simple criteria, the candidate were selected and indicated in the same table (Table 2). We found 9 out of 18 (50 per cent of) our sample are considered as candidates. The recent observation of Kraus et al. (2005) (which was not known to authors at the time of our observation: April–May, 2004) confirms that USco 65 and USco 66 are multiple systems, and USco 109 is most likely a multiple system. In our RV-shift tests, we found all the multiples confirmed by Kraus et al. (2005) in our multiple candidates. Further they found USco 67, 128, 130, 132 as non-multiple, and similarly we found them as 'non-candidates' for multiplicity. The discrepancy between their results and ours are only in USco 75 and USco 112. While our results suggests that these are candidates for multiple systems, Kraus et al. (2005) did not find them as multiple systems. This difference may be caused by the difference in sensitivity (on a binary separation) of the two different methods. Another possible caused of the difference is that the uncertainties in RVs may be underestimated, since surface activity of the objects may also contribute noise in the RV measuements; however, the levels of th noise is expeted be small for BD and VLM stars (c.f. Joergens 2006b).

Table 2. Summary of the observations, the heliocentric radial velocities (RV) from two-epoch and the average rotational velocities ($v \sin i$). The uncetainties of relative radial velocties ($\sigma_{\rm RRV}$) with respect to the template star LHS 049 and the average radial velocties ($\overline{\rm RV}$) are also given. The last column indicates whether a target is a candidate for multiplicity i.e. the measured radial velocity changes from two different epoch is larger than $1\,\sigma_{\rm RRV}$ of each others (c.f. Fig. 1).

Object	Date	MDJ-2453100	RV $[\mathrm{km\,s^{-1}}]$	$\sigma_{\rm RRV}$ $[\mathrm{km\,s^{-1}}]$	$\overline{\rm RV}$ $[\mathrm{km\,s^{-1}}]$	$v \sin i$ $[\mathrm{km\,s^{-1}}]$	candidate?
GY 5	2004-Apr-25	20.22051	-6.14 ± 0.84	0.68			
	2004-May-08	33.27776	-5.96 ± 0.60	0.34	-6.05 ± 1.03	16.5 ± 0.6	no
GY 141	2004-May-11	36.16016	-4.39 ± 0.60	0.34			
	2004-May-18	43.15707	-2.95 ± 0.51	0.11	-3.67 ± 0.79	4.4 ± 1.4	yes
GY 310	2004-Apr-25	20.32700	-4.83 ± 0.74	0.54			
	2004-May-10	35.31139	-8.43 ± 0.51	0.11	-6.63 ± 0.90	11.1 ± 6.0	yes
USco 40	2004-Apr-06	01.25900	-7.15 ± 0.74	0.54			
	2004-May-08	33.25324	-6.80 ± 0.51	0.11	-6.98 ± 0.90	34.2 ± 0.5	no
USco 53	2004-Apr-05	00.39651	-7.27 ± 0.93	1.21			
	2004-May-03	28.23079	-5.43 ± 0.74	0.55	-6.35 ± 1.19	40.0 ± 0.6	no
USco 55	2004-Apr-06	01.33509	-5.39 ± 0.50	0.02			
	2004-May-03	28.30546	-6.38 ± 0.53	0.27	-6.38 ± 0.73	22.9 ± 0.8	yes
USco 66	2004-Apr-06	01.29007	-5.32 ± 0.57	0.29			
	2004-May-03	28.28683	-6.41 ± 0.65	0.42	-5.87 ± 0.86	25.9 ± 1.2	no
USco 67	2004-Apr-06	01.21481	-6.01 ± 0.74	0.55			
	2004-May-03	28.21759	-6.83 ± 0.59	0.31	-6.42 ± 0.90	18.4 ± 0.4	no
USco 75	2004-Apr-05	00.37453	-6.75 ± 0.67	0.44			
	2004-May-08	33.09532	-9.88 ± 1.94	1.88	-8.32 ± 2.05	55.6 ± 3.0	yes
USco 100	2004-Apr-06	01.30836	-6.76 ± 2.74	2.69			
	2004-May-03	28.26425	-10.23 ± 1.80	1.73	-8.47 ± 3.28	43.7 ± 3.2	no
USco 101	2004-Apr-05	00.30191	-4.22 ± 0.87	0.71			
	2004-May-03	28.14804	-6.07 ± 0.69	0.48	-5.15 ± 1.11	19.1 ± 0.3	yes
USco 104	2004-Apr-05	00.27545	-5.83 ± 0.50	0.02			
	2004-May-03	28.12391	-7.48 ± 0.50	0.06	-6.66 ± 0.06	16.7 ± 0.4	yes
USco 109	2004-Apr-06	01.23587	-4.15 ± 0.52	0.16			
	2004-May-08	33.11929	-4.41 ± 0.50	0.03	-5.12 ± 0.72	8.6 ± 1.2	yes
USco 112	2004-Apr-05	00.34486	-2.70 ± 0.69	0.47			
	2004-May-08	33.07139	-3.46 ± 0.51	0.11	-3.08 ± 0.86	5.8 ± 1.2	yes
USco 121	2004-Apr-25	20.19466	-39.47 ± 0.51	0.11			
	2004-May-03	28.18537	-42.43 ± 0.50	0.02	-40.95 ± 0.71	17.6 ± 1.3	yes
USco 128	2004-May-14	39.28595	-7.41 ± 0.85	0.69			
	2004-May-18	43.09885	-6.94 ± 1.16	1.05	-7.18 ± 1.44	3.6 ± 1.1	no
USco 130	2004-May-10	35.26060	-4.83 ± 0.54	0.21			
	2004-May-14	39.34201	-4.95 ± 0.74	0.55	-4.89 ± 0.92	15.2 ± 1.1	no
USco 132	2004-May-12	37.28394	-7.18 ± 0.58	0.30			
	2004-Jun-18	43.12719	-7.37 ± 1.02	0.89	-7.28 ± 1.17	9.1 ± 0.7	no

Finally, the histogram of the RVs using only the objects in USco OB is given in Figure 2. The total number of the objects is 14. Note that USco 121 is excluded from the graph since it is identified as a non-member of the UScOB association based on the RV value (see Table 2). Muzerolle et al. (2003) also found it to be a likely non-member based on the radial velocity and the low lithium abundance. The distribution of the RVs in the figure was fitted by a gaussian function. We found that the standard deviation and the peak position of the radial velocity distribution are $1.2\,\mathrm{km\,s^{-1}}$ and $-5.9\,\mathrm{km\,s^{-1}}$ respectively. The former is very similar to the standard deviation ($0.9\ \mathrm{km\,s^{-1}}$) of the radial velocity distribution of 9 BDs and VLM objects in Cha I found by Joergens (2006a). They also studied the radial velocity distribution of more massive 25 T Tauri stars in Cha I, and found the standard deviations ($1.3\,\mathrm{km\,s^{-1}}$) is not significantly different from that of the brown dwarfs and the very low-mass objects. Unfortunately, we do not have the radial velocity measurements of the higher mass counter parts (T Tauri stars) in Upper Sco OB association. This is also planned for a near future investigation as this is important for the study of the mass dependency of the kinematics in a young stellar cluster.

According to the hydrodynamical simulations of a low-mass star-forming cluster of Bate et al. (2003) which yields a stellar density of $1.8 \times 10^3\,\mathrm{stars\,pc^{-3}}$, the rms dispersion (1-D) of the stars and the BDs is $1.2\,\mathrm{km\,s^{-1}}$. Similarly for the model with a higher stellar density ($2.6 \times 10^3\,\mathrm{stars\,pc^{-3}}$), the rms dispersion is 2.5 $\mathrm{km\,s^{-1}}$ (Bate 2005). The standard deviation of $\overline{\rm RV}$ ($1.2\,\mathrm{km\,s^{-1}}$) found in our analysis is more comparable the lower stellar density model.

3.2 Rotational velocities

The rotational velocities of the objects were determined by measuring the widths of the cross correlation curves of the target spectra against a template spectrum from an object which is known to have a very small rotational velocity. The line broadening of the targets is assumed to be dominated by rotational broadening. As in the cases for the radial velocity measurements, LHS 49 is chosen for

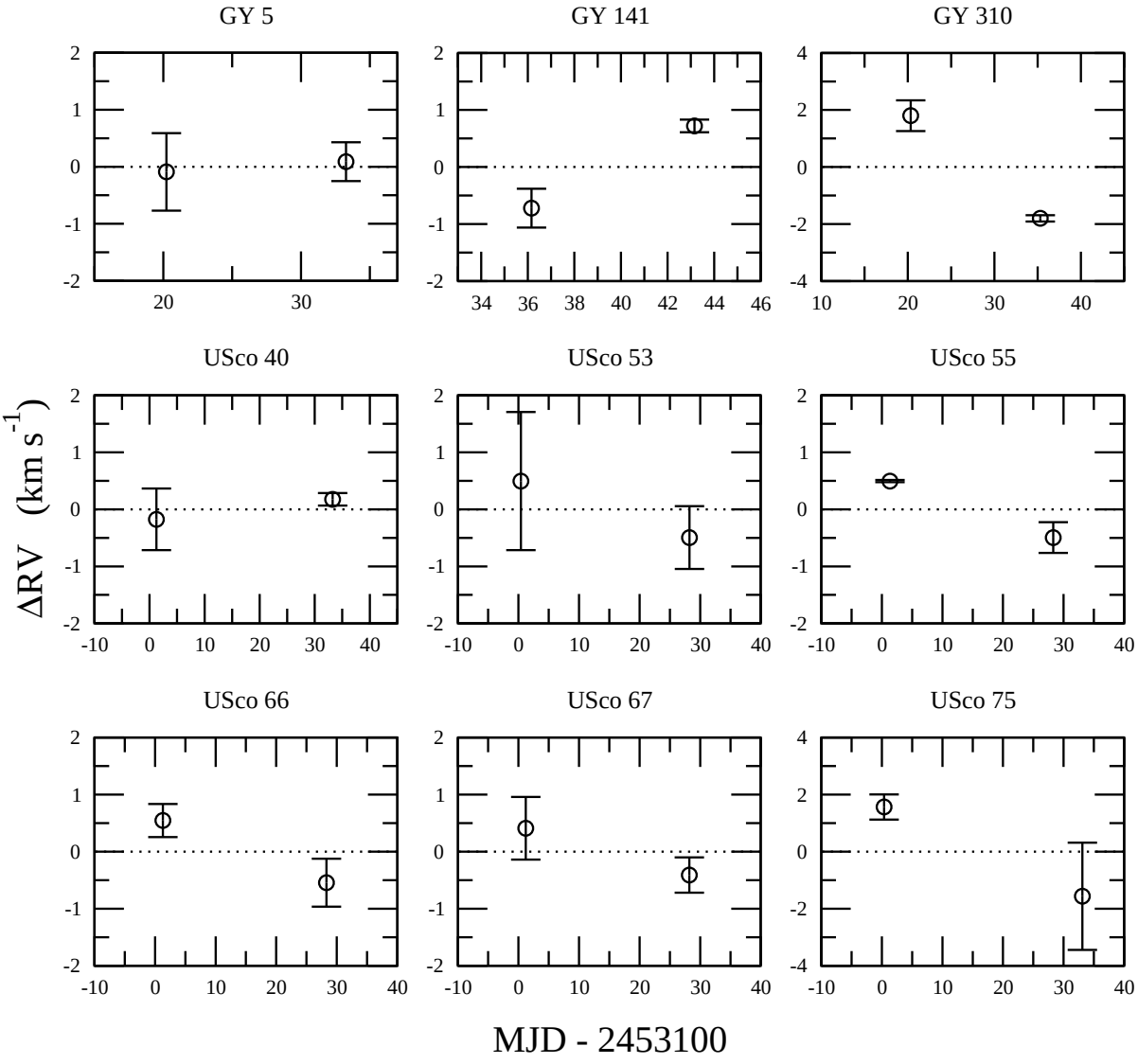

Figure 1. Relative radial velocities (RVs) of objects measured in two different epochs. The vertical axes indicate the amount of deviation (ΔRV) from the 'average' radial velocitiy ($\overline{\rm RV}$) in Table 2), and the horizontal axes indicate the time of the observation in modified Julian date (MJD; XXX do you really mean MJD rather than heliocentric JD????). The objects are considered to have a non-constant RV when the error bars of two data points do not overlap each other. The non-constant RV objects are considered as binary/multiple candidates.

the template. Using its known period ($P \approx 83\,{\rm d}$, Benedict & et al. 1998) and radius ($R_* \approx 0.145\,{\rm R}_\odot$ from the VLTI measurement by Ségransan et al. 2003), the rotational velocity of LHS 49 is estimated as $v \sin i = 2\pi R_*/P \approx 0.1\,{\rm km\,s^{-1}}$; hence, negligibly small.

The width of the cross-correlation curves ($\sigma_{\rm CCF}$) are calibrated with the rotational velocities ($v \sin i$) by cross correlating the template spectra against the same template spectra with added rotation (convolved with a given $v \sin i$), as similarly done by e.g. Tinney & Reid (1998), Mohanty & Basri (2003) and White & Basri (2003). The linear limb-darkening law with a solar-like parameter ($\epsilon = 0.6$) was assumed in the formulation of the rotational profile described by Gray (1992), his Eq. 17.12. For each object, two measurements of rotational velocities are computed from two independent spectra obtained at different epochs. As similary done for the RV measurements, the mean and the standard deviation of the mean are used as the final rotational velocity and its uncertainty. The final results are placed in Table 2. In general, our measurements are in good agreement with the earlier measurements of Muzerolle et al. (2003) and Mohanty et al. (2005), given in Table 2. For example, Muzerolle et al. (2003) found $v \sin i = 16.8 \pm 2.7\,{\rm km\,s^{-1}}$ for GY 5 while we found $v \sin i = 16.5 \pm 0.6\,{\rm km\,s^{-1}}$.

The range of $v \sin i$ found among our objects is 3.6–$55.6\,{\rm km\,s^{-1}}$, and a similar range is also found by Mohanty et al. (2005). The left panel of Figure 2 shows the histogram of $v \sin i$ distribution for the UScoOB objects (14 objects excluding USco 121, non member). The log-normal fit of this distribution gives the peak position at $16.9\,{\rm km\,s^{-1}}$ and the standard deviation $\sigma = 27.8\,{\rm km\,s^{-1}}$. Using the $v \sin i$ data in Joergens & Guenther (2001), the same histogram bin size used for UScoOB obects and the log-normal fit, we find the $v \sin i$ distribution of the BD and VLM stars (8 objects) in Cha I peaks at $15.4\,{\rm km\,s^{-1}}$, and has the standard deviation of $8.0\,{\rm km\,s^{-1}}$. The peak of the distribution is

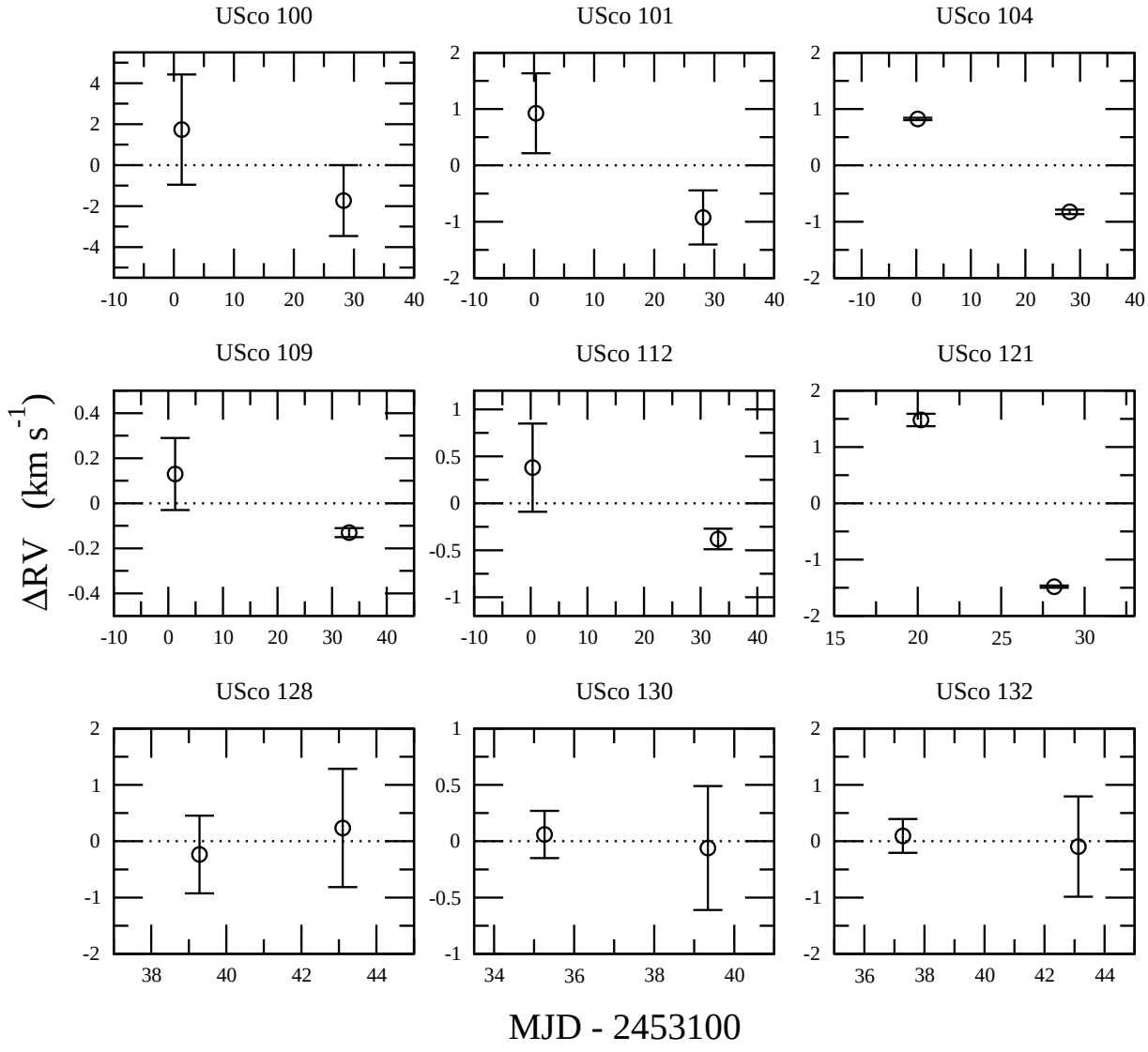

Figure 1. continued

similar to that of Upper Sco objects, but the standard deviation of the distribution is significantly smaller than that of the Upper Sco objects. The difference maybe due to the very small number of samples. A similar fit was applied to the $v \sin i$ distribution of 14 T Tauri stars in Cha I using the data of Joergens & Guenther (2001), and we found the peak at $17.0\,\mathrm{km\,s^{-1}}$ and the standard deviation $25.9\,\mathrm{km\,s^{-1}}$ which are very similar to those of the Upper Sco brown dwarf candidate objects.

4 BINARY FREQUENCY

According to Table 2, 9 out of 18 (50 per cent of) samples are considered as binary/multiple candidates. The fraction slightly decreases to 43 per cent (6 out of 14) if we consider the objects only in the UScoOB. These fractions are significantly larger than the binary fraction (25 per cent, 3 out of 12) found by the recent high-resolution imaging survey of brown dwarfs and very low-mass objects (M5.5–M7.5) in the UScoOB (Kraus et al. 2005). The imaging surveys are sensitive to wider binaries (separation$\gtrsim 4\,\mathrm{au}$) while our technique is more sensitive to narrower ($\lesssim 1\,\mathrm{au}$) or shorter period ($\sim 10\,\mathrm{d}$) binaries. However, our RV-shift test also detected all the binaries found in the imaging survey of Kraus et al. (2005), demonstrating that the method is also effective in the systems with a separation 5–18 au. In Section 3.1, we have found all the binaries confirmed by Kraus et al. (2005) also as our binary/multiple candidates. In addition to those samples commonly found, we have two more candidates (USco 75 and USco 112) which are in the sample of Kraus et al. (2005), but not detected as binaries by them. If we assume these objects are real binary/multiple systems but not detected by the imaging survey because of possibly very small separations, their multiplicity fraction would increase to 5 out of 9 (56 per cent) which is more consistent with the fraction suggested by our RV survey.

Another possible reason for the different binary fraction suggested by our data is that the uncertainties in the RV values may be underestimated. Since the our suggested binary fraction is merely that for the binary 'candidates', the follow-up RV monitoring of the candidates must be done to confirm the true multiplicity, and to determined firmer constraint on the binary/multiple faction in

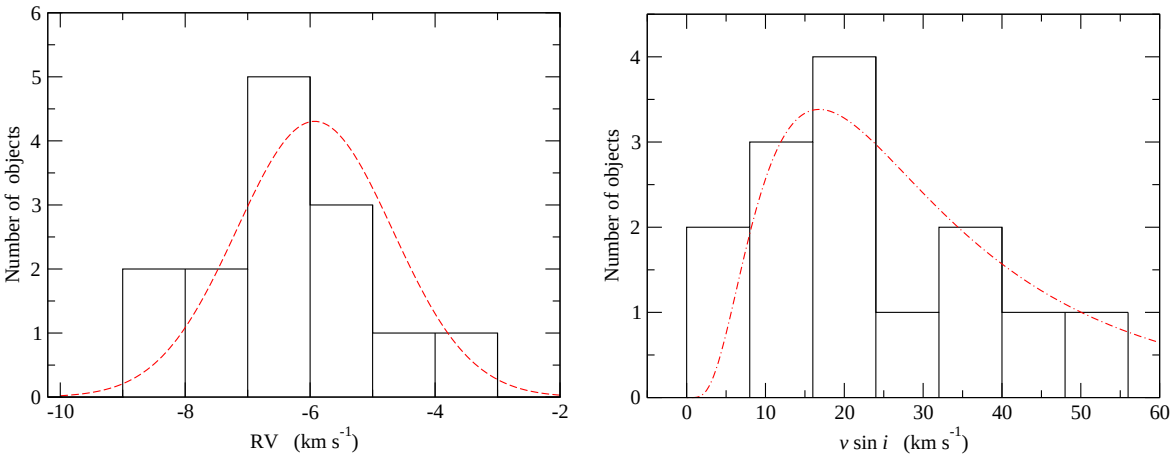

Figure 2. Histogram of the average heliocentric radial velocities (left) and the rotational velocities (right) of 14 UScoOB BD and VLM objects listed in Table 2 (excluding USco 121, a non-member). The gaussian fit (dashed line) of the radial velociity distribution gives a standard deviation of $1.2\,\mathrm{km\ s^{-1}}$ and the peak position of $-5.9\,\mathrm{km\ s^{-1}}$. The log-normal fit (dash-dot) of the rotational velocity distribution gives a standard deviation $27.8\,\mathrm{km\ s^{-1}}$ and the peak poistion $16.9\,\mathrm{km\ s^{-1}}$.

the UScoOB. This is planned for a near future. The binary fraction of slightly more massive pre-main-sequence stars was studied by Köhler et al. (2000) using the K-band speckle interferometry of X-ray selected samples. For the UScoOB members with spectral type M0–M5 (0.7–0.13 $\mathrm{M}_{\odot}$), they found the binary fraction of $52\,(\pm10)$ per cent (26 out of 50) with the separation 21–1000 au. On the other hand, Köhler et al. (2000) found no wide ($> 20\,\mathrm{au}$) binary in their survey, and suggested that there may be a discontinuity in separation distribution around $M_{*} \sim 0.1\,\mathrm{M}_{\odot}$.

A similar imaging survey of the brown dwarf candidates in Cha I cloud by Neuhäuser et al. (2002) and Neuhäuser et al. (2003) also found the multiplicity rate $\lesssim 10\,\mathrm{per\,cent}$ using 12 objects (Cha Hα 1–12 with M6–M8). Using a subset of the same sample and the same radial velocity technique used in this paper, Joergens (2006b) found only 11 per cent (1 out of 9) of the sample showed non-constant RVs in her multi-epoch data, indicating a much smaller multiplicity fraction. It is unclear at this moment whether the difference is caused by the physical nature of the two different star forming regions.

5 CONCLUSIONS

We have presented two-epoch RV survey of 18 young BDs and VLM stars in UScoOB and ρ Oph dark cloud core using the high resolution UVES echelle spectroscopy at VLT. The amount of the shifts in RVs in time is used to identify the candidates for multiplicity.

We found 9 out of 18 objects (50 per cent) are possible candidates in this analysis. For the objects in UScoOB, we found 6 out of 14 objects (43 per cent) as candidates. Compared to the average binary fraction ($\sim 20\,\mathrm{per\,cent}$) of magnitude-limited imaging surveys for BDs and VLM stars (M6 and later) in the field (c.f. Burgasser et al. 2006), the fraction of the binary 'candidates' found by this RV survey is significantly higher. The possible reasons to for the discrepancy are: (1) caused by the different sensitivity on the binary separation in the imaging and RV technique, (2) caused by possibly under estimated uncertainties in the measured RV values. The true multiplicity of the candidates must be confirmed by follow-up spectroscopy monitoring of candidates.

We found a good agreement with the high resolution imaging survey of the BD and VLM objects in UScoOB of Kraus et al. (2005). All three confirmed binaries in UScoOB by Kraus et al. (2005) are found as the multiplicity candidate this RV survey; however, we found two objects (USco 75 and USco 112) also as binary candidates while they found them as singles.

From the distribution of RV values in UScoOB, we confirmed that USco 121 is most likely a non-member of the association, as similarly found so by Muzerolle et al. (2003). We found the RV dispersion of the objects in UScoOB is very similar to that of the BDs and VLM stars in Chamaeleon I (Cha I) previously studied by others. The rotational velocities ($v\,\sin i$) of the samples are also measured. The distribution of $v\,\sin i$ for the UScoOB objects peaks around $16.9\,\mathrm{km\ s^{-1}}$ which is similar to that of the Cha I population.

The follow-up spectroscopic observations of the binary candidates presented here are planned in near future. There are only a few RV variable binary candidates are identified from the earlier surveys (Guenther & Wuchterl 2003; Kenyon et al. 2005; Joergens 2006b). As Burgasser et al. (2006) pointed out most of the current RV and imaging surveys use samples from magnitude-limited survey, but one should attempt to use the samples from volume-limited survey in order to find a correct statistics on binary parameters more straight forwardly, i.e. without correcting for bias.

ACKNOWLEDGEMENTS

This work is supported by PPARC rolling grant PP/C501609/1. We thank the staff of VLT of the ESO for the observations carried out in the service mode.

References

Ardila D., Martín E., Basri G., 2000, AJ, 120, 479
Bailer-Jones C. A. L., 2004, A&A, 419, 703
Baranne A., Queloz D., Mayor M., Adrianzyk G., Knispel G., Kohler D., Lacroix D., Meunier J.-P., Rimbaud G., Vin A., 1996, A&AS, 119, 373

Basri G., Martín E. L., 1999, AJ, 118, 2460
Bate M. R., 2005, MNRAS, 363, 363
Bate M. R., Bonnell I. A., Bromm V., 2002, MNRAS, 332, L65
—, 2003, MNRAS, 339, 577
Benedict G. F., et al., 1998, AJ, 116, 429
Bouy H., Moraux E., Bouvier J., Brandner W., Martín E. L., Allard F., Baraffe I., Fernández M., 2006, ApJ, 637, 1056
Burgasser A. J., McElwain M. W., Kirkpatrick J. D., 2003, AJ, 126, 2487
Burgasser A. J., Reid I. N., Siegler N., Close L., Allen P., Lowrance P., Gizis J., 2006, ArXiv Astrophysics e-prints
Close L. M., Siegler N., Freed M., Biller B., 2003, ApJ, 587, 407
de Zeeuw P. T., Brown A. G. A., de Bruijne J. H. J., Hoogerwerf R., Lub J., Le Poole R. S., Blaauw A., 1997, in ESA SP-402: Hipparcos - Venice '97, pp. 495–500
de Zeeuw P. T., Hoogerwerf R., de Bruijne J. H. J., Brown A. G. A., Blaauw A., 1999, AJ, 117, 354
Duquennoy A., Mayor M., 1991, A&A, 248, 485
García-Sánchez J., Weissman P. R., Preston R. A., Jones D. L., Lestrade J.-F., Latham D. W., Stefanik R. P., Paredes J. M., 2001, A&A, 379, 634
Gizis J. E., Reid I. N., Knapp G. R., Liebert J., Kirkpatrick J. D., Koerner D. W., Burgasser A. J., 2003, AJ, 125, 3302
Gray D. F., 1992, The Observation and Analysis of Stellar Photospheres. Cambridge Univ. Press, Cambridge, UK
Guenther E. W., Wuchterl G., 2003, A&A, 401, 677
Joergens V., 2006a, A&A, 448, 655
—, 2006b, A&A, 446, 1165
Joergens V., Guenther E., 2001, A&A, 379, L9
Kenyon M. J., Jeffries R. D., Naylor T., Oliveira J. M., Maxted P. F. L., 2005, MNRAS, 356, 89
Köhler R., Kunkel M., Leinert C., Zinnecker H., 2000, A&A, 356, 541
Kraus A. L., White R. J., Hillenbrand L. A., 2005, ApJ, 633, 452
Luhman K. L., Rieke G. H., 1999, ApJ, 525, 440
Martín E. L., Barrado y Navascués D., Baraffe I., Bouy H., Dahm S., 2003, ApJ, 594, 525
Maxted P. F. L., Jeffries R. D., 2005, MNRAS, 362, L45
Mohanty S., Basri G., 2003, in The Future of Cool-Star Astrophysics: 12th Cambridge Workshop on Cool Stars, Stellar Systems, and the Sun (2001 July 30 - August 3), eds. A. Brown, G.M. Harper, and T.R. Ayres, (University of Colorado), 2003, p. 683-688., Brown A., Harper G. M., Ayres T. R., eds., pp. 683–688
Mohanty S., Jayawardhana R., Basri G., 2005, ApJ, 626, 498
Muzerolle J., Hillenbrand L., Calvet N., Briceño C., Hartmann L., 2003, ApJ, 592, 266
Neuhäuser R., Brandner W., Alves J., Joergens V., Comerón F., 2002, A&A, 384, 999
Neuhäuser R., Guenther E., Brandner W., 2003, in IAU Symposium, Martín E., ed., p. 309
Padoan P., Nordlund Å., 2002, ApJ, 576, 870
Pinfield D. J., Dobbie P. D., Jameson R. F., Steele I. A., Jones H. R. A., Katsiyannis A. C., 2003, MNRAS, 342, 1241
Reipurth B., Clarke C., 2001, AJ, 122, 432
Ségransan D., Kervella P., Forveille T., Queloz D., 2003, A&A, 397, L5
Tinney C. G., Reid I. N., 1998, MNRAS, 301, 1031
Udry S., Mayor M., Queloz D., 1999, in ASP Conf. Ser. 185: IAU Colloq. 170: Precise Stellar Radial Velocities, Hearnshaw J. B., Scarfe C. D., eds., p. 367
White R. J., Basri G., 2003, ApJ, 582, 1109
Whitworth A. P., Zinnecker H., 2004, A&A, 427, 299
Wilking B. A., Greene T. P., Meyer M. R., 1999, AJ, 117, 469